RESEARCH PAPER

Human Vaccines & Immunotherapeutics 11:5, 1129–1139; May 2015; © 2015 Taylor & Francis Group, LLC

Comparable quality attributes of hepatitis E vaccine antigen with and without adjuvant adsorption-dissolution treatment

Yue Zhang[1,2], Min Li[1,3], Fan Yang[1,3], Yufang Li[1,3], Zizheng Zheng[1,3], Xiao Zhang[1,3], Qingshan Lin[1,2], Ying Wang[4], Shaowei Li[1,2,3], Ningshao Xia[1,2,3], Jun Zhang[1,3,*], and Qinjian Zhao[1,3,*]

[1]State Key Laboratory of Molecular Vaccinology and Molecular Diagnostics; National Institute of Diagnostics and Vaccine Development in Infectious Diseases; Xiamen University; Xiamen, Fujian, PR China; [2]School of Life Science; Xiamen University; Xiamen, Fujian, PR China; [3]School of Public Health; Xiamen University; Xiamen, Fujian, PR China; [4]China National Center for Biotechnology Development; Beijing, PR China

Keywords: aluminum-based adjuvant, binding analysis, capsid protein, epitope integrity, hepatitis E virus, monoclonal antibodies

Most vaccines require adjuvants for antigen stabilization and immune potentiation. Aluminum-based adjuvants are the most widely used adjuvants for human vaccines. Previous reports demonstrated the preservation of antigen conformation and other antigen characteristics after recovery from adjuvanted Hepatitis B and human papillomavirus vaccines. In this study, we used a combination of various physiochemical and immunochemical methods to analyze hepatitis E vaccine antigen quality attributes after recovery from adjuvants. All biochemical and biophysical methods showed similar characteristics of the p239 protein after recovery from adjuvanted vaccine formulation compared to the antigen in solution which never experienced adsorption/desorption process. Most importantly, we demonstrated full preservation of key antigen epitopes post-recovery from adjuvanted vaccine using a panel of murine monoclonal antibodies as exquisite probes. Antigenicity of p239 was probed with a panel of 9 mAbs using competition/blocking ELISA, surface plasmon resonance and sandwich ELISA methods. These multifaceted analyses demonstrated the preservation of antigen key epitopes and comparable protein thermal stability when adsorbed on adjuvants or of the recovered antigen post-dissolution treatment. A better understanding of the antigen conformation in adjuvanted vaccine will enhanced our knowledge of antigen-adjuvant interactions and facilitate an improved process control and development of stable vaccine formulation.

Introduction

Hepatitis E virus (HEV) is a major cause of sporadic and epidemic hepatitis and HEV leads to an annual 14 million symptomatic infections worldwide.[1] HEV infection accounts for acute-on-chronic liver failure, predominantly in patients from Indian subcontinents and other developed countries.[2] High morbidity and mortality among pregnant women are characteristic identifiers of waterborne epidemic outbreaks of hepatitis E, including outbreaks in South Sudan, Uganda and Nepal in recent years.[3] In 2011, an efficacious prophylactic vaccine Hecolin® was licensed in China to meet this unmet medical need.[4] Hecolin® is based on recombinant p239 VLPs expressed in *E. coli* and adsorbed on aluminum (Al)- based adjuvants, as previously described.[5,6 7] The largest randomized, controlled phase III vaccine trials to date using this recombinant vaccine was conducted in Jiangsu Province, China, and enrolled 112,604 healthy adult participants.[8–10] A vaccine efficacy of approximately 79.2% (95% confidence interval [CI], 67.7% to 86.6%) in the prevention of infection was demonstrated with greater protection rate against clinical illness.[10,11] Another HEV vaccine based on recombinant HEV viral capsid protein was also tested clinically, demonstrating high efficacy against HEV infection and disease. [12,13 14]

The above-mentioned Hecolin® contains aluminum-based adjuvants for enhancing the antigen immunogenicity. [15,16] Aluminum-containing adjuvants were widely adopted in vaccine formulations for human use over the past several decades due to their capability for potentiating humoral responses against administered antigens and their excellent safely profile. An assay for the completeness of antigen adsorption to particulate adjuvants is generally performed in vaccine formulations as part of the process control and product consistency process. Complete antigen adsorption, which is the case for commercial recombinant protein based vaccines such as for Hepatitis B or HPV, is generally preferred for better process control and for antigen stabilization. The mechanisms of antigen binding to aluminum salts have been previously reported, including electrostatic and hydrophobic attraction and ligand exchange of antigen phosphate groups.[17–19] Electrostatic attraction is the most powerful force between an antigen molecule and particulate adjuvants.[18,20]

*Correspondence to: Jun Zhang; Email: zhangj@xmu.edu.cn; Qinjian Zhao; Email: qinjian_zhao@xmu.edu.cn
Submitted: 08/03/2014; Revised: 10/24/2014; Accepted: 11/08/2014
http://dx.doi.org/10.1080/21645515.2015.1009343

While the antigen adsorption process and mechanism have been studied, the analysis on adsorbed protein in adjuvanted vaccines has been rarely reported due to potential morphological structure changes, thermal stability variations and alterations of epitope structure. Therefore, a better understanding of antigen conformation/structure when adsorbed onto adjuvants and of antigens once desorbed from the particulate adjuvants is desired for assuring vaccine potency and stability.

Various antigen desorption or adjuvant dissolution methods were used to elute antigens off particulate adjuvants or to recover antigens via desorption of aluminum-based adjuvants.[21] No significant changes were observed in protein antigens eluted from the aluminum-containing adjuvants using optimized antigen recovery methods including the use of chelating agents and surfactants.[18,22–24]

Cryo-transmission electron microscopy (Cryo-EM) and binding analyses of VLP antigens in GARDASIL®, the quadrivalent human papillomavirus (HPV) VLP vaccine, showed no apparent changes in their spherical shape and key epitopes of VLP antigens when adsorbed onto adjuvants and after dissolution of amorphous adjuvants.[25,39] Comparable physiochemical properties of the recovered HBsAg antigen of Hepatitis B virus versus the antigen in aqueous solution were shown using multiple biophysical methods.[22] The purpose of the studies was to explore the interactions between proteins and the aluminum-containing adjuvants and to provide guidance for the production of more consistent and stable vaccine formulations.[24] In addition, a full recovery antigen enables the *in vitro* potency assay development for vaccine lot release and stability testing.[39]

This work demonstrated the consistency of the physicochemical and immunochemical properties of the HEV p239 protein antigen in Hecolin® in an aqueous solution vs. the recovered antigen after adsorption-dissolution treatment. This work focuses on the antigen characterization on pre- and post-dissolution treatment and full recovery of the p239 antigen was observed after adjuvant dissolution. A combination of non-overlapping, orthogonal methods were employed to demonstrate comparable quality attributes, particularly antibody binding activities using a panel of monoclonal antibodies (mAbs), for the p239 protein with and without adsorption-dissolution treatment.

Results

Recombinant p239-based VLPs in Hecolin® before adsorption and after dissolution were characterized using different methods for detailed antigen characteristics analysis. Full recovery (101% ± 1%, n = 3) of protein based on a UV method was observed post adjuvant dissolution. The methods and results are summarized in **Table 1**, which shows the multiplicity in analytical methodology. These multifaceted analyses of the antigen showed the consistent properties of the p239 in its native state and after desorption from adjuvants, which indicated no alterations in key epitopes of the antigens recovered from adjuvanted vaccine formulation.

No alterations in antigen morphology or thermal stability

Thermal stability using differential scanning calorimetry

Vaccine stability is a critical factor for a viable vaccine product. Thermal-induced unfolding of a protein antigen is somewhat related to actual vaccine stability. The thermal stability of the native p239 VLPs in solution (Sample a) and the (Sample c) was comparable as indicated by similar T_m values (approximately 75°C) (**Fig. 1B**). No change was discernible between native VLPs and post-adjuvant dissolution-recovered p239 VLPs. The tertiary and quaternary structure of the protein were maintained in the recovered antigens from adjuvanted vaccines based on the similar melting profiles and T_m values. Interestingly, the melting temperature (T_m) of the aluminum-adsorbed p239 VLPs (Sample b, 77.2°C) was slightly higher.

Transmission electron microscopy and dynamic light scattering

TEM was used to visualize overall morphology and TEM and DLS were used to assess size distribution of the particles to determine the size and morphology of the p239 in aqueous solution versus the antigens recovered post-dissolution (**Fig. 1A, C**). The HEV p239-based VLPs (Samples a, c and c_0) in solution showed sizes of 27.2, 27.2, 26.1 nm on average in diameters by DLS (**Table 1**), which is in agreement with results on multiple p239 batches in aqueous solution previously reported.[7]

High performance size-exclusion chromatography

The retention times in HPSEC for native and post-adjuvant dissolution-recovered p239 VLPs (Samples a, b and c_0) were nearly identical. The similar size and comparable homogeneity of the p239 VLPs in Samples a, b and c_0, as displayed by HPSEC profiles, (**Fig. 2A**) was consistent with the TEM and DLS result in the above section.

Analytical ultracentrifugation

AUC was used to determine the hydrodynamic radius and assess the homogeneity of native p239 VLPs and post-adjuvant dissolution recovered p239 VLPs. The almost identical sedimentation peak for Samples a (21.8 s), c (20.5 s) and c_0 (20.6 s) demonstrated the comparable hydrodynamic behavior of the p239 VLPs regardless of the treatment process (**Fig. 2B**).

Isoelectric point (pI) analysis and integrity of p239

Normalized isoelectric focusing analysis of native p239 VLPs and post adjuvant dissolution recovered p239 VLPs showed nearly identical pI values for p239 in Samples a, c and c_0 with different treatments under native conditions (**Fig. 2C**). SDS-PAGE assessment could reveal any potential degradation, including the purity and integrity of the p239 VLPs in different preparations. Only a single band was observed which showed the integrity of p239 in the 3 samples with no proteolytic clipping during absorption/desorption treatment under denaturing conditions (data were not shown).

Epitope mapping (9 × 9) for p239 VLPs

A panel of 9 mAbs, chosen based on the non-overlapping information revealed and data elucidated through analysis by

Table 1. Comprehensive characterization of HEV p239 VLPs of antigen in aqueous solutions versus post-adsorption onto aluminum containing adjuvant and dissolution treatment to demonstrate comparable product attributes

		Parameters of p239 in different conditions			
		Sample a	**Sample b**	**Sample c**	**Sample c_0**
Method	**Charateristics**	**Native p239 VLPs**	**Adsorbed p239 VLPs**	**HEV vaccine dissolution**	**p239 in dissolution mixture**
	Biophysical and biochemical methods				
HPSEC[a]	size (reflected by retention time, min)	13.7	—	13.8 (20.0*)	13.8 (20.1*)
TEM	morphology	particulate antigen ~(20–30 nm in diameters)			
DSC[b]	thermal stability (T_m, °C)	75.0 ± 0.1	77.2 ± 0.2	75.2 ± 0.1	75.4 ± 0.4
AUC	sedimentation coefficient (S)	21.3 ± 0.5	—	20.8 ± 0.8	20.6 ± 0.5
DLS	hydrodynamic diameter (nm)	27.2	—	27.2	26.1
SLS[c]	hydrodynamic diameter (μm)		10.29		
icIEF	isoelectric point (pI)	5.85 ± 0.03 (n = 3)	—	5.80 ± 0.04 (n = 3)	5.83 ± 0.03 (n = 3)
	Immunochemical methods				
Cross-inhibitory assay[e]	inhibitory capability	inhibitory capability by 9 mAbs from each other for different samples (Sample a, c and c_0) showed by heat map (**Fig. 3**).			
SPR[e]	binding to mAbs	binding activity to 6 mAbs for different samples (Sample a, c and c_0) with relative antigenicity (**Fig. 4**).			
Sandwich ELISA[d]	antigenicity (rEC_{50})	1.00 (n = 3)	—	1.21 ± 0.01 (n = 3)	1.14 ± 0.07 (n = 3)

[a]An analytical TSK Gel PW5000xl (7.8 mm × 300 nm) column (TOSOH, Tokyo, Japan) was used in the HPSEC analysis."*" 20 min is a buffer peak.
[b]DSC was applied to the recombinant protein-based vaccine characterization, which reflects the thermal stability of sample.[33] During the process of heating, protein in the solution tended to aggregate. The melting temperature was detected 3 times, and it is shown as an average.
[c]The aluminum hydroxide was 11.3 ± 0.1 μm (n=3), the size of the mix compound (p239 adsorbed to aluminum hydroxide) was similar to the aluminum hydroxide with no statistically significant differences (**Fig. 1C** and **Table 1**).
[d]Sandwich ELISA was used to detect the antigenicity of the different antigens (a, c and c_0) in this assay. The capture antibody was 3A11 and the detection antibody was 8C11-HRP.
[e]Although no numeric data are being reported here, the methods are listed for the completeness of the analytical toolbox and full results are presented in **Figures 3 and 4**.

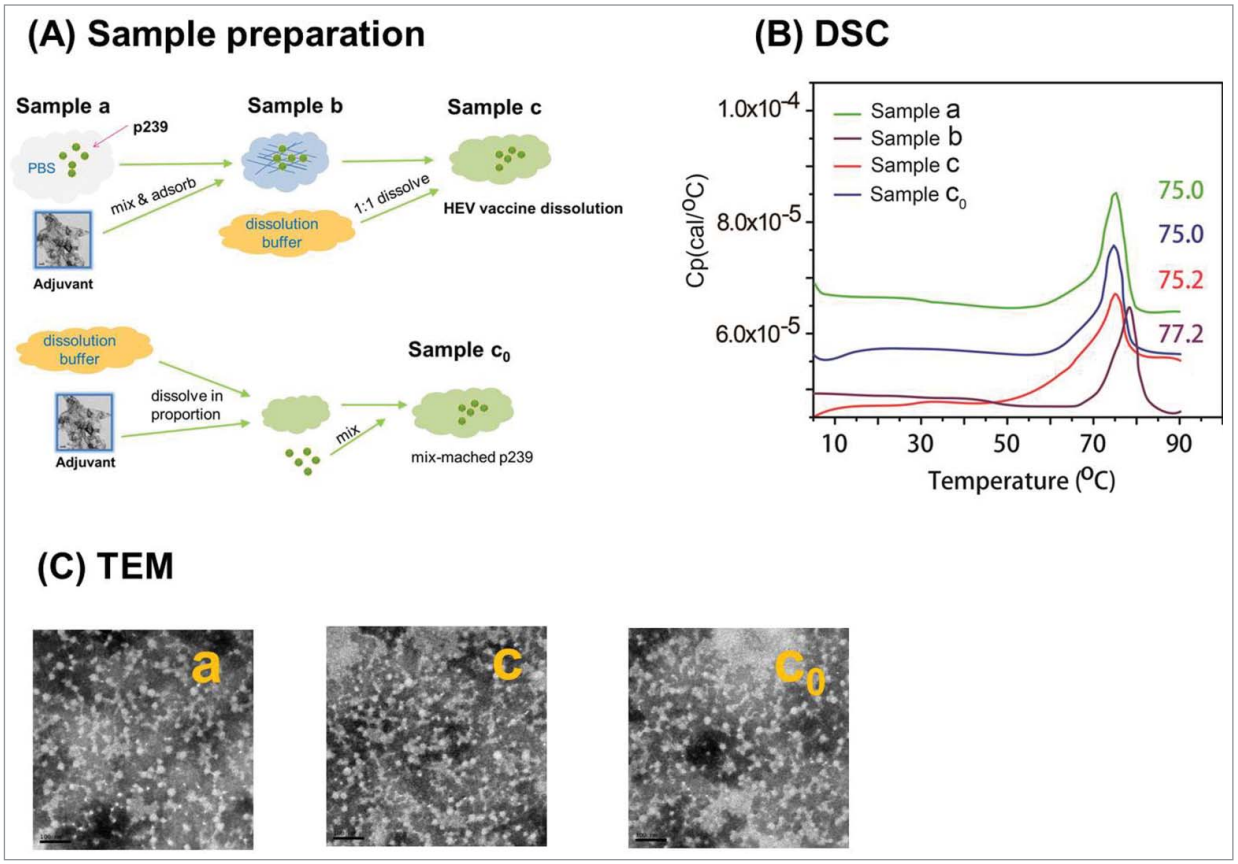

Figure 1. The sample preparation and consistent profiles of p239 vaccine antigen particles detected by DSC and TEM. (**A**) The samples were prepared according to the flow diagram. The process shows the preparation of p239 VLPs in Samples a, c, and c_0 that were used for multiple analyses, with Sample c_0 being the matrix-matched control for Sample c. (**B**) Comparable thermal stability as shown by DSC profiles – similar transition temperatures (between 75°C to 75.2°C) were obtained for p239 VLPs in Samples a, c and c_0, and a slightly higher transition temperature (77.2°C) was observed in absorbed p239 VLPs in Sample b. (**C**) Morphology of p239 VLPs were examined using transmission electron microscopy (TEM). The spherical particles of native (Sample a) and aluminum-dissolved p239 VLPs (Samples c and c_0) presented similar morphology (Bar = 100 nm).

different mAbs, were used for pairwise epitope mapping using cross-blocking ELISA (**Fig. 3A and B**). Six of these mAbs recognize conformational epitopes (8G12, 12F12, 8C11, 12A7, 13D8 and 9F7) and 3 mAbs recognize linear epitopes (15B2, 12A10 and 3A11). The approximate relationship between epitopes is illustrated in **Figure 3**A. Cross-blocking between these 9 mAbs analyzed the relative location or degree of overlap for these specific epitopes on p239 in different samples. Using multiple epitope approach increases the confidence in antigen characterization and in assuring product consistency as in the case for HPV vaccines.[32–34]

The higher detection limit of the blocking rate was identified as 95% because the lower limit of ELISA value is 0.05, and the value of no blocking group was controlled between 1.0 and 1.5. Three more level of blocking rates (50%, 75% and 90%) identified the relationship between each blocking and detection antibody (**Fig. 3B**).

In general, the results of mAb cross-blocking showed the relative position of 2 mAbs that recognized epitopes on the surface of p239 in different samples (**Fig. 3B**). A higher blocking rate indicated more similar positioning of the 2 epitopes on the protein. Highly analogous mAb cross-blocking profiles (9 × 9) were observed in the cross-blocking results for p239 in aqueous solution (Sample a) and p239 recovered from adjuvanted vaccine formulation (Sample c), which indicated no changes in the epitopes of the recovered antigen after dissociation of the adjuvant and 239 protein (**Fig. 3B**). Sample c_0 is the matrix-matched control of Sample c, which was not subjected to the adsorption-dissolution process. The heat maps of Sample c and Sample c_0 showed certain subtle differences in the blocking rates of 3A11, 8G12, 8C11 against 15B2 and 12A10. However, the blocking rate heat maps of all 3 samples shown in **Figure 3B** showed high degree similarities, indicating no discernible changes of antigen conformation based on mAb binding profiles. The mAb-based epitope mapping data showed that the relative location of the epitopes of the p239 antigen were not altered by the adjuvant and post dissolution treatment.

One-site antigenicity measurement with multiple mAbs

One-site binding and label-free assays with 6 representative murine mAbs (8G12, 8C11, 13D8, 12F12, 3A11 and 12A10) for p239 antigen in 3 samples were measured using SPR. The six

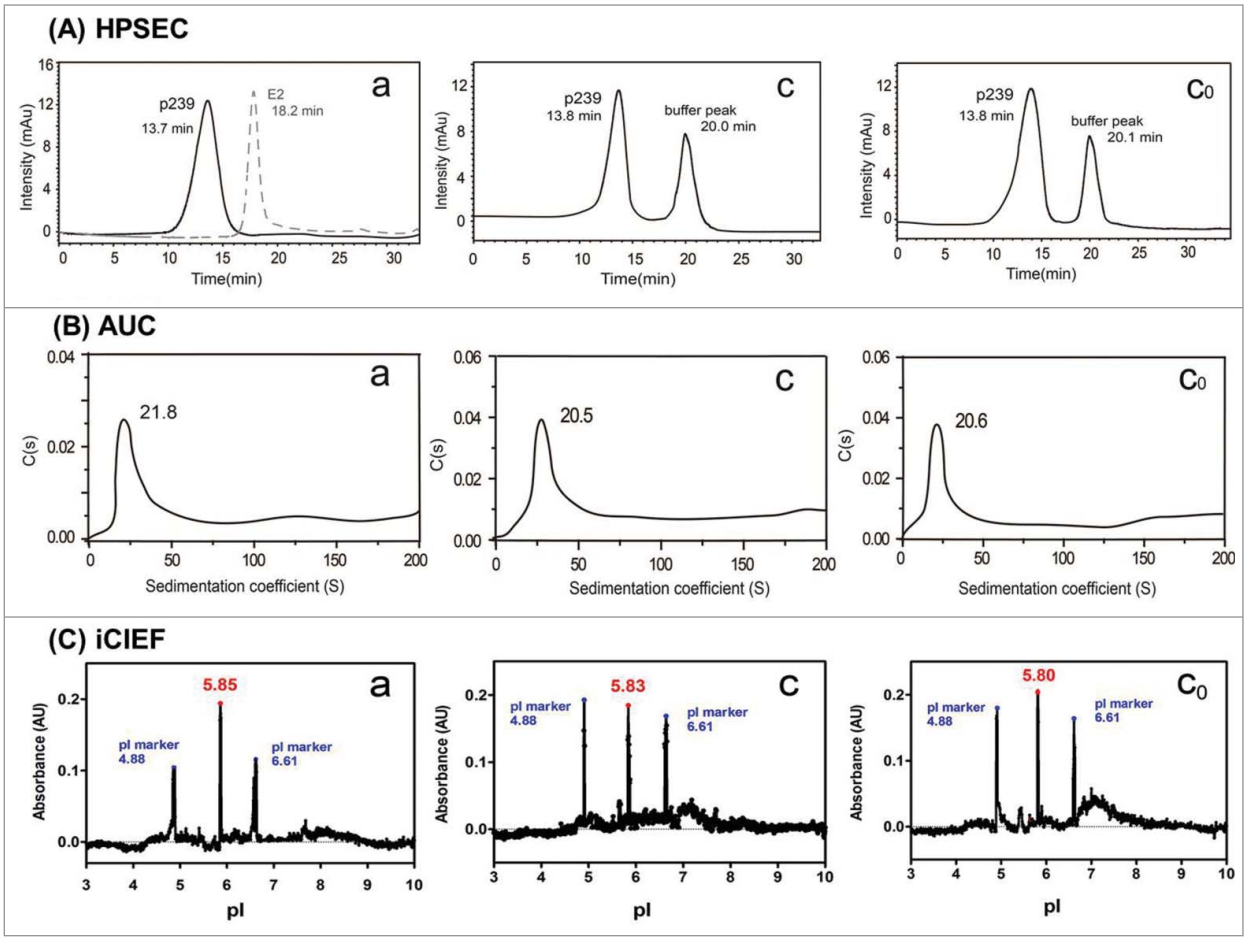

Figure 2. Consistent characteristics of p239 VLPs in Samples a, c and c_0) undergoing different treatments. (**A**) HPSEC showed consistent antigen particle size (nearly identical retention time for Samples a, c and c_0). The molecular weight of p239 and E2 (dimer) were approximately 3,162 kDa and 147 kDa, respectively.[7] Dimer, E2, in the assay serves as a control for elution pattern for a dimeric molecule, as opposed to a particulate antigen.[28] (**B**) AUC profiles revealed similar coefficients (21.8 s – 20.5 s) for p239 in 3 different samples. (**C**) Analogous pI (5.80 – 5.83) values of native and desorbed p239 VLPs were demonstrated by iCIEF.

mAbs, which recognize different epitopes, were used to evaluate the immuno reactivity of p239 in Samples a, c and c_0, reflecting mAb binding activities to different epitopes. Four of the 6 mAbs used (8C11, 8G12, 13D8 and 12F12) recognize distinct conformational epitopes and mAbs 3A11 and 12A10 recognize 2 different linear epitopes. The rationale for mAb choice and detailed mAb characterization and epitope mapping will be published separately in the future. The distinct epitopes for 4 mAbs (8C11, 12F12, 3A11 and 12A10) are illustrated to show the orthogonality of the information from the binding analyses using these mAbs (**Fig. 4B**). The RU ratio for p239 VLPs ($\triangle RU_{Ag}$) binding to a given amount of captured mAbs ($\triangle RU_{Ab}$) was tracked (rRU = $\triangle RU_{Ag}/\triangle RU_{Ab}$). The relative antigenicity was calculated by normalizing the rRU value of each sample (Samples a, c and c_0) to the native p239 VLP (Sample a) (**Table 1** and **Fig. 4A**) and the range of relative antigenicity for each mAb was within 0.9 to 1.2. Multiple mAbs, recognizing different epitopes, were used to probe binding activities, and the results revealed that no major modifications occurred on the surface of the p239 VLPs during the adsorption and desorption processes. The orthogonality of the information on antigen epitopes from these binding assays was illustrated in **Figure 4B** showing the epitopes for different mAbs.[7]

The mAb-based 2-site antigenicity measurement

Most commonly used ELISA is sandwich ELISA with ruggedness and robustness needed in a manufacturing setting. Thus, binding activity to a neutralizing mAb (such as 8C11), serving as a surrogate marker for clinical efficacy, can be probed in a robust and easy-to-perform assay (**Fig. 5A**). A sandwich ELISA was used to assess the p239 antigenicity in Samples a, c, and c_0. Based on the results (**Table 1** and **Fig. 5B**), relative EC_{50} (EC_{50} of Sample c or Sample c_0/EC_{50} of Sample a) was used to measure the relative binding activity for Samples a, c and c_0. All three samples showed good binding profiles in ELISA with 3A11 as capture Ab and 8C11 as detection Ab. Comparable antigenicity (based on the EC_{50} values) for the 3 samples was observed, and relative EC_{50} value was well within the $\pm$ 20% of the reference sample (Sample a).

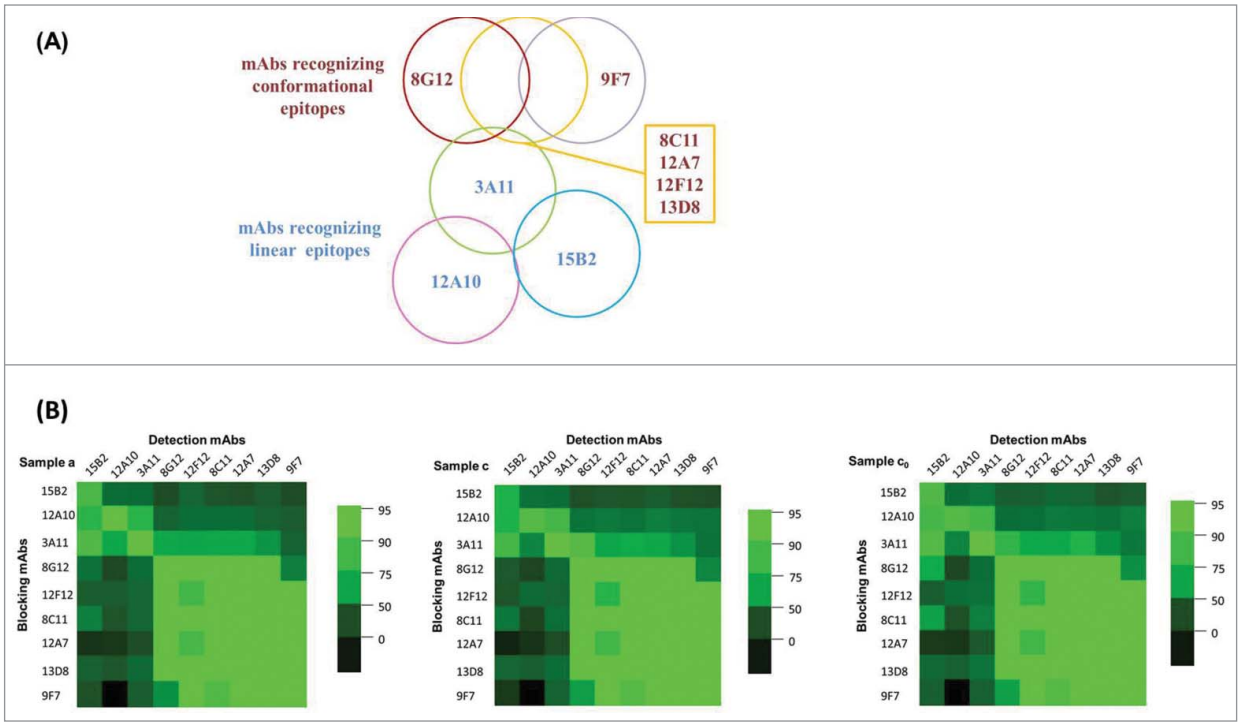

Figure 3. Epitope mapping (9 × 9) using monoclonal antibodies for the comparable epitope overlap of HEV p239 in different samples. (**A**) The illustration of the epitope overlap for 9 mAbs. While four mAbs, 8C11, 12A7, 12F12, 13D8, recognized epitopes in a similar region. Their affinity and footprint sizes differed significantly (Zheng, ZZ, unpublished results). (**B**) The horizontal character is representative of a monoclonal antibody with an HRP enzyme, and longitudinal characters represent non-enzyme monoclonal antibodies. Each small grid represents the results of a monoclonal antibody blocking against an HRP-conjugated monoclonal antibody. Color gradient represents the change in blocking rate: green represents a blocking rate of more than 95%, and black represents a blocking rate is 0.

Discussion

This work employed a mild dissolution method to dissolve the aluminum-based adjuvants and release the p239 protein (an antigen in Hecolin®) for analysis. The native, adsorbed and post-adjuvant dissolution recovered p239 protein were examined using multi-faceted techniques to characterize the properties of p239 in 4 vaccine antigen preparations (**Fig. 1A** and **Table 1**). Full recovery of the intact p239 antigen from aluminum-based adjuvants was demonstrated by a UV based method, while the

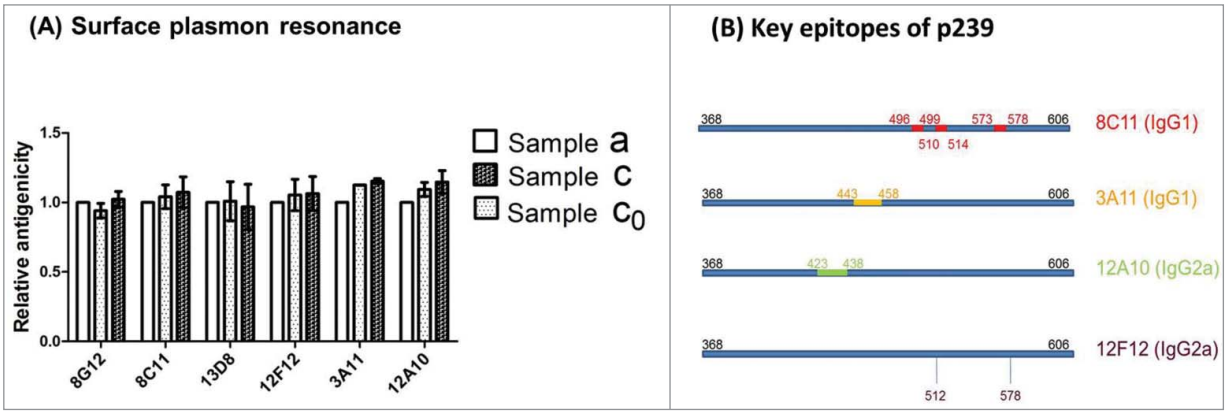

Figure 4. Comparable antigenicity of different HEV p239 VLP samples was determined using an SPR method with 6 different mAbs. (**A**) The RU ratio for p239 VLPs ($\triangle RU_{Ag}$) binding to a given amount of captured mAbs ($\triangle RU_{Ab}$) was tracked ($rRU = \triangle RU_{Ag}/\triangle RU_{Ab}$). The relative antigenicity was calculated by normalizing the rRU value of each sample (Samples a, c and c_0) to the native p239 VLP (Sample a). (**B**) The key conformational and linear epitopes on the surface of HEV p239 VLPs recognized by different mAbs are illustrated.

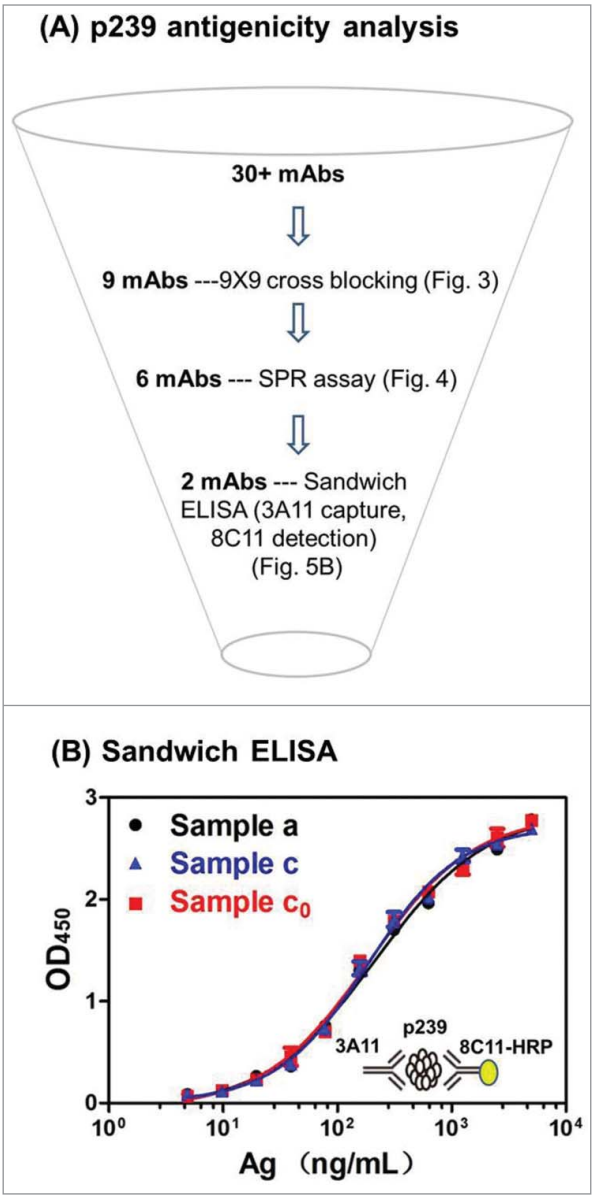

Figure 5. Immunochemical assays for p239 multi-faceted antigenicity analysis and comparable antigenicity by a sandwich ELISA. (**A**) mAb characterization and their applications in epitope mapping, SPR assay and sandwich ELISA for p239 antigenicity analysis. (**B**) The antigenicity of different p239 VLPs (Samples a, c and c_0) were measured using a monoclonal antibody-based sandwich ELISA (3A11 as the capture antibody, with 8C11 as the detection antibody). EC_{50} values for different samples are reported in **Table 1**.

method tracking the bulk properties of antigen such as HPSEC, DLS and AUC, etc, showed no alteration on particle hydrodynamic behaviors and size distribution. Preservation of key epitopes on p239 antigen post-dissolution treatment was confirmed using immuno-reactivity to different monoclonal antibodies.

Among the numerous adjuvants being studied, the aluminum-based adjuvants are widely used for human vaccines. We investigated whether an HEV VLP antigen maintained native-like conformations when adsorbed onto particulate adjuvants and post-dissolution treatment. Recently, Greiner et al. showed that adsorption through a ligand exchange of phospholipids from HBsAg particles with hydroxyl groups from aluminum-based adjuvants damaged the integrity of the external lipid layer of the particles and lead to a rearrangement of the S proteins.[22] In addition, Lyer et al. noted that vaccines exhibiting different degree of adsorption, namely 3, 35 and 85%, changed to 40% within 1 h after exposure to interstitial fluid. Interestingly, similar antibody titers were observed for all 3 formulations, regardless of the initial degree of antigen adsorption. It was concluded that immunopotentiation by aluminum-containing adjuvants correlated to the degree of antigen adsorption in interstitial fluid at the injection site rather than in the vaccine formulation.[35,36]

However, how a given vaccine exerts its function may be more closely related to the desorbed antigen, which can be taken up by dendritic cells or other antigen-presenting cells via phagocytosis and pinocytosis. Multiple mechanisms of antigen elution were described, including the disruption of electrostatic, hydrophobic interactions, phosphate exchange, protein denaturation and dissolution of aluminum hydroxide.[18,24] One hypothesis was proposed that during desorption behavior, an altered adsorption mechanism from electrostatic attractive forces to ligand exchange would decrease the desorption efficacy of the aged ovalbumin model antigen. In contrast, desorption efficacy did not change in an aged lysozyme model vaccine because the only adsorption mechanism was electrostatic forces.[37] In addition, Jendrek et al. indicated that the point of zero charge of the aluminum adjuvant approaches the point of zero charge of a protein antigen, and this decrease in the charge differential between the 2 species in a complex is reduced, leading to the release of the antigen.[18,38] Therefore, proper dissolution conditions, most likely antigen-specific, may be developed to remove antigens from adjuvants for morphological and antigenicity analyses.[39]

Different dissolution/desorption conditions could result in different yields or quality of antigen recovery from vaccine products. The recombinant HBsAg particles in a Hepatitis B vaccine were fully recovered from adjuvanted vaccines because of the mild eluting conditions. Comparable physiochemical properties of the recovered antigen vs. the native particles were demonstrated using a combination of various techniques.[22,40] In addition, Zhao et al. reported that the morphology of the GARDASIL® VLPs was unaffected by adjuvants using visual inspection and a tomographic method. The VLPs in GARDASIL® were desorbed using a citrate phosphate buffer, and a full recovery of the antigenicity of mAb-based analysis was observed after adjuvant dissolution.[25,39] This technique enabled the development of an *in vitro* relative potency assay to replace the animal-based potency assay for product release and stability testing.[39] In contrast, Tleugabulova et al. reported a denaturation of HBsAg particles after desorption from aluminum adjuvant under harsher conditions, which led to irreversible modifications of the particles likely as a result of much stronger interaction between phospholipids in HBsAg particles and adjuvants.[41]

Most of the dissolution studies on vaccine formulation were performed *in vitro*, but several reports noted that similar

phenomena occur *in vivo* after vaccine injection due to the antigen desorbing capability of interstitial fluid. In one specific case, aluminum adjuvant-adsorbed tetanus toxoid and HIV-gp 120 injected *in vivo* were rapidly released from the injection site.[42,43] This result is consistent with antigen desorption when exposed to interstitial fluid.[37]

Most importantly, the desorbed antigen from the aluminum adjuvants should be assessed using various methods with specific mAbs to demonstrate the integrity of different epitopes. Using multiple epitope approach for analysis on recombinant vaccine antigens is critical in increasing the confidence of the epitope integrity of recombinant antigens. This is also a common practice in analytics for human vaccines.[30–35] Among the mAbs used for the HEV antigen, the most critical mAb is a protective and neutralizing antibody, mAb 8C11. MAb 8C11 recognizes conformational epitopes that are composed of 3 discontinuous peptide segments in a dimeric form of the truncated HEV capsid protein. Most importantly, 8C11 effectively captures authentic HEV virions.[28] Therefore, the binding activity to 8C11 is a surrogate marker of virion-like epitopes on recombinant VLPs and vaccine efficacy in the generation of protective and neutralizing antibodies.[28] Therefore, 8C11 can be used in different ways as a useful molecular probe for antigen quality assessment, such as *in vitro* relative potency determinations as the detection or revealing Ab in a sandwich ELISAs, as in the case for HPV vaccine Gardasil® (with neutralizing H16.V5 as the detection antibody).[28,39] Also, 8C11 can be an effective probe for the label-free analysis of Ab-Ag interactions using a sensor-chip based assay with short assay turn-around time. Similar sensor chip-based assays were used for VLP-based hepatitis B vaccine with RF1 and A1.2.[40,44] Regardless one-site or 2-site assays, binding activity to the neutralizing and protective mAb, such as 8C11, could be used as a surrogate marker for vaccine efficacy.[28] With these analytical toolbox in place and with the in vitro potency test being developed in particular, vaccine stability, accelerated or real time stability, will be addressed in future publications for Hecolin as there could be a need in the future of transporting the vaccine to the needed areas such as in a refugee camp without cold chains.

A comprehensive analytical toolbox is critically important for structural and functional analyses of vaccines. Among these assays, the potency assay is most critical for vaccine characterization and lot-release testing. Sandwich ELISA with good reproducibility and robustness, it could be a candidate *in vitro* relative potency assay for product release once implemented in a manufacturing setting. In the case for HPV vaccines, mouse potency assay and a whole set of in vitro testing assays were used for HPV vaccine Gardasil® and Cervarix® for process control and product comparability.[34,39,45] While animal-based assays are still being use for vaccine characterization, the progress of the vaccinology, robust vaccine production procedures, improved characterization methods and the development of well-characterized vaccines create possibilities to reduce animal use during vaccine development and vaccine manufacturing. Replacement of *in vivo* tests for batch release of actual vaccines is difficult, but emerging technologies are providing more chances to use well-considered reductions of *in vivo* experiments during product and process development and improvement.[46-47] A proposal called '3R' (replace, reduce and refine) has been put forward that every effort should be made to reduce animal use and to decrease the animal distress to a minimum in each experiment.[48] Therefore, more alternative *in vitro* experiments, such as the methods presented here, sandwich ELISA, SPR and the others could be implemented to minimize animal use throughout the life cycle management of a licensed vaccine.

In conclusion, a combination of various techniques was used to demonstrate the preservation of HEV p239 (antigen in Hecolin®) conformation on adjuvants and recovered antigens post-dissolution treatment. Multifaceted and orthogonal methods demonstrated the lack of alterations in particle morphology, protein stability and key epitopes of this recombinant VLP-based antigen. To characterize antigens recovered from adjuvanted vaccines, this report describes a concept and toolbox that should be applicable to other vaccines, particularly vaccines with recombinant proteins as antigens.

Materials and Methods

Recombinant p239 VLPs and adjuvants

Recombinant p239 VLPs were expressed in *E. coli* and purified to a homogeneity of high purity as indicated in SDS-PAGE with quantitative analysis done with a densitometer (over 99%).[6] Concentrations of purified p239 were measured using BCA method. Adjuvants were colloidal aluminum hydroxide and prepared in-house. The shelf life of prefilled syringes for Hecolin was 24 Mo at 4°C, and this was extended to 36 Mo recently based on stability data.

Monoclonal antibodies (mAbs)

A panel of 9 anti-HEV p239 murine mAbs (8C11, 8G12, 13D8, 12F12, 3A11, 15B2, 9F7, 12A7 and 12A10, all IgG subclass) were prepared in-house as previously reported.[26 27] The mAbs were affinity-purified from ascites fluid using a Protein A column. Concentrations of purified murine mAbs were determined using OD at 280 nm.[28] Purified mAbs were labeled with horse radish peroxidase (HRP) using a standard periodate conjugation method for antibody conjugation in ELISA as previously described.[7,27]

Adsorption/desorption process

Aluminum hydroxide (to a final concentration of 0.554 mg Al/mL) was mixed with p239 VLPs (200 μg/mL) in phosphate buffer (40 mM) at pH 7.4 for antigen adsorption. The mixture was allowed to sit at 4°C for at least 24 hours. For dissolution, the completely adsorbed sample was gently mixed 1:1 (by volume) with the dissolution buffer (0.1 M citrate and 0.2 M phosphate, pH 6.0). The mixture was incubated with mixing at 200 rpm using a constant shaking incubator (Zhicheng Co., Shanghai, China) for 24 hours at room temperature to dissolve adjuvants and to recover antigens. A matrix-matched sample was also included in all analyses for comparison purposes. A flow chart of sample preparation is shown in **Figure 1A**. Then, the

concentration of the recovered protein post-adjuvant dissolution was determined with OD at 280 nm using a UV method with a Multiscan* Go microplate reader/spectrophotometer (Thermo Scientific, Utah, US).

Particle size analysis

Transmission electron micrograph (TEM)

The morphologies of p239 VLPs undergoing different treatment processes (Samples a, b, c and c_0) were examined with negative staining using a JEM2100HC transmission electron microscope (JEOL, Tokyo, Japan) operated at 200 kV. The p239 VLPs were diluted to 100 μg/mL and stained with 2% uranyl acetate after excess fluid removal.

Dynamic light scattering (DLS)

The hydrodynamic size distribution of the p239 VLPs (at 200 μg/mL) was measured using a Dynapro-MS/X DLS system (Protein Solution, Joplin, MO), as previously described.[7] The radius of the p239 VLPs (Samples a, c and c_0) was calculated using the Stokes-Einstein equation, and each reported value is an average of 20 acquisitions for each measurement.

Static light scattering (SLS)

A LS13320 laser particle analyzer (Beckman Coulter, Miami, FL) equipped with an optical bench and a Universal Liquid Module was used to measure the size distribution of adjuvanted p239 VLP vaccine suspended in ddH_2O at 20°C.[29] No difference was observed in particle size when either saline or ddH_2O was used as diluent during analysis.

High performance size-exclusion chromatography (HPSEC)

The size of the particulate p239 antigen was analyzed using an analytical TSK Gel PW5000xl (7.8 mm × 300 nm) column (TOSOH, Tokyo, Japan) under native conditions as previously described.[8]

Isoelectric point (pI) determination

The whole column imaging method of capillary isoelectric focusing (iCIEF) was used to demonstrate the isoelectric point (pI) of the p239 VLPs. The operating system and reagents were all provided by the vendor (Advanced Electrophoresis Solutions Ltd, Ontario, Canada). The isoelectric focusing solution (0.35% methylcellulose and 8% ampholyte, pH 3–10), catholyte (0.1 M NaOH in 0.1% methylcellulose), anolyte (0.1 M phosphoric acid in 0.1% methylcellulose) and pI markers were used in this study. The signal of final running sample containing 400 μg/mL p239 VLPs was detected at 280 nm from Samples a, c and c_0. The pI in each sample was determined by the relative distance from peaks for the 2 pI makers (pI 4.88 and pI 6.61) with 3 independent replicate measurements.

Analytical ultracentrifugation (AUC)

Sedimentation velocity (SV) experiments were performed using a Beckman XL-A analytical ultracentrifuge equipment (Beckman Coulter, Fullerton, CA) at 20°C to characterize the homogeneity and hydrodynamic behaviors of the p239 VLPs. Samples with a concentration of 0.5 OD were centrifuged at 15,000 rpm. The sedimentation coefficient was obtained using the c (s) method using Sedfit software, which was generous provided by Dr. P. Schuck (National Institutes of Health).

Thermal stability by differential scanning calorimetry (DSC)

Differential scanning calorimetry (DSC) was performed using a MicroCal VP-DSC instrument (GE Healthcare, MicroCal Products Group, Northampton, MA) to determine the energy of protein unfolding transitions induced by the heating of p239 protein. All samples were diluted to 100 μg/mL and measured as previously reported.[7]

Immuno reactivity to murine mAbs

Epitope analyses based on cross-blocking of anti-HEV mAbs

Micro well plates were coated with 100 ng/well p239 protein (Samples a, c or c_0) at 37°C for 2 hours and blocked with 0.5% (w/v) casein in phosphate-buffered saline (PBS) at 37°C for 2 hours. After five times washes, 50 μg/well blocking antibodies were added and incubated at 37°C for 1 hour. HRP-conjugated detection antibodies were diluted in PBS containing 20% BSA to a concentration that resulted in a final OD value between 1.0 and 1.5 in an indirect ELISA and added to the blocking antibody incubated plates at 37°C for another 30 min. The plates were incubated with 100 μl tetramethylbenzidine substrate for 10 min at 37°C after 5 washes. The reaction was stopped by the addition of 50 μl 2 M H_2SO_4, and the OD was measured at 450 nm (against OD at 630 nm as background). The blocking rate was calculated as the percentage of the decreased OD value of the blocked well compared to the OD value in the unblocked control well.

Surface plasma resonance (SPR)

A surface plasmon resonance binding assay was performed using a Biacore 3000 instrument (GE Healthcare) with different mAbs and the similar procedures as previous described to assess the epitope-specific antigenicity of the p239 VLPs in different samples (Sample a, c and c_0).[30,31] Six different murine mAbs (8C11, 8G12, 13D8, 12A10, 3A11 and 12F12) were first captured by the immobilized goat-anti-mouse IgG Fc (GAM-Fc) on the chip surface in PBS running buffer. Subsequently, p239 antigen in Samples a, c and c_0 was flowed through the chip surface with the captured mAbs. The RU ratio (or rRU) for p239 VLPs ($\triangle RU_{Ag}$) binding to a given amount of captured mAbs ($\triangle RU_{Ab}$) was tracked ($rRU = \triangle RU_{Ag}/\triangle RU_{Ab}$). For a given mAb, the relative antigenicity was calculated by normalizing the rRU value of each sample (Samples c and c_0) to the native p239 VLP (Sample a) (**Table 1**).

Sandwich ELISA

A mAb-based sandwich ELISA was used to evaluate the antigenicity of the p239 VLPs (Samples a, c and c_0) by tracking 2 different epitopes. The 96-well microplates were coated with the mAb 3A11 to capture p239 antigen (serial dilutions, starting concentration of 5 ug/mL) and the 8C11-HRP was used as the detection antibody. EC_{50} values were calculated using GraphPad

Prism (GraphPad Software, San Diego, CA) by fitting the ELISA data using a 4-parameter logistic fit.

Disclosure of Potential Conflicts of Interest

No potential conflicts of interest were disclosed.

Funding

This research was supported by the China Ministry of Health and Family Planning via the Major Project (2013ZX0910101), National Science Fund (81373061), and Institute Reconstruction Fund (2011FU125Z04).

References

1. Perez-Gracia MT, Mateos Lindemann ML, Caridad Montalvo Villalba M. Hepatitis E: current status. Reviews in medical virology 2013; 23:384–98
2. Haim-Boukobza S, Coilly A, Sebagh M, Bouamoud M, Antonini T, Roche B, Yordanova O, Savary J, Saliba F, Duclos-Vallee JC, et al. Hepatitis E infection in patients with severe acute alcoholic hepatitis. Liver Int: Off J Int Assoc Study Liver 2014; in press http://dx.doi.org/10.1111/liv.12610
3. Wu T, Zhu FC, Huang SJ, Zhang XF, Wang ZZ, Zhang J, Xia NS. Safety of the hepatitis E vaccine for pregnant women: a preliminary analysis. Hepatology 2012; 55:2038; PMID:22161542; http://dx.doi.org/10.1002/hep.25522
4. Zhang J, Shih JW, Wu T, Li SW, Xia NS. Development of the hepatitis E vaccine: from bench to field. Semin Liver Dis 2013; 33:79-88; PMID:23564392; http://dx.doi.org/10.1055/s-0033-1338116
5. Wu T, Li SW, Zhang J, Ng MH, Xia NS, Zhao QJ. Hepatitis E vaccine development A 14-year odyssey. Hum Vacc Immunother 2012; 8:823-7; PMID:22699438; http://dx.doi.org/10.4161/hv.20042
6. Ma Y, Lin SQ, Gao Y, Li M, Luo WX, Zhang J, Xia NS. Expression of ORF2 partial gene of hepatitis E virus in tomatoes and immunoactivity of expression products. World J Gastroentero 2003; 9:2211-5
7. Zhang X, Wei M, Pan H, Lin Z, Wang K, Weng Z, Zhu Y, Xin L, Zhang J, Li S, et al. Robust manufacturing and comprehensive characterization of recombinant hepatitis E virus-like particles in Hecolin. Vaccine 2014; 32:4039-4050; PMID:24892250; http://dx.doi.org/10.1016/j.vaccine.2014.05.064
8. Li SW, Zhang J, Li YA, Ou SH, Huang GY, Huang GY, He ZQ, Ge SX, Xian YL, Pang SQ, et al. A bacterially expressed particulate hepatitis E vaccine: antigenicity, immunogenicity and protectivity on primates. Vaccine 2005; 23:2893-901; PMID:15780738; http://dx.doi.org/10.1016/j.vaccine.2004.11.064
9. Zhu FC, Zhang J, Zhang XF, Zhou C, Wang ZZ, Huang SJ, Wang H, Yang CL, Jiang HM, Cai JP, et al. Efficacy and safety of a recombinant hepatitis E vaccine in healthy adults: a large-scale, randomised, double-blind placebo-controlled, phase 3 trial. Lancet 2010; 376:895-902; PMID:20728932; http://dx.doi.org/10.1016/S0140-6736(10)61030-6
10. Krain LJ, Nelson KE, Labrique AB. Host immune status and response to hepatitis E virus infection. Clin Microbiol Rev 2014; 27:139-65; PMID:24396140; http://dx.doi.org/10.1128/CMR.00062-13
11. Zhang J, Zhang XF, Zhou C, Wang ZZ, Huang SJ, Yao X, Liang ZL, Wu T, Li JX, Yan Q, et al. Protection against hepatitis E virus infection by naturally acquired and vaccine-induced immunity. Clin Microbiol Infect: Off Pub Eur Soc Clin Microbiol Infect Dis 2014; 20:O309-405; PMID:24112138; http://dx.doi.org/10.1111/1469-0691.12257
12. Kamili S. Toward the development of a hepatitis E vaccine. Virus Res 2011; 161:93-100; PMID:21620908; http://dx.doi.org/10.1016/j.virusres.2011.05.008
13. Myint KSA, Gibbons RV. Hepatitis E: a neglected threat. T Roy Soc Trop Med H 2008; 102:211-2; PMID:17658568; http://dx.doi.org/10.1016/j.trstmh.2007.03.014
14. Shrestha MP, Scott RM, Joshi DM, Mammen MP Jr, Thapa GB, Thapa N, Myint KS, Fourneau M, Kuschner RA, Shrestha SK, et al. Safety and efficacy of a recombinant hepatitis E vaccine. New Engl J Med 2007; 356:895-903; PMID:17329696; http://dx.doi.org/10.1056/NEJMoa061847
15. Shirodkar S, Hutchinson RL, Perry DL, White JL, Hem SL. Aluminum compounds used as adjuvants in vaccines. Pharmaceut Res 1990; 7:1282-8; http://dx.doi.org/10.1023/A:1015994006859
16. Heimlich JM, Regnier FE, White JL, Hem SL. The in vitro displacement of adsorbed model antigens from aluminium-containing adjuvants by interstitial proteins. Vaccine 1999; 17:2873-81; PMID:10438058; http://dx.doi.org/10.1016/S0264-410X(99)00126-7
17. A bacterially expressed particulate hepatitis E vaccine: antigenicity im, J. V., White JL, Hem SL. Effect of pH on the elution of model antigens from aluminum-containing adjuvants. J Colloid Interf Sci 1998; 205:161-5; PMID:9710509; http://dx.doi.org/10.1006/jcis.1998.5648
18. Jendrek S, Little SF, Hem S, Mitra G, Giardina S. Evaluation of the compatibility of a second generation recombinant anthrax vaccine with aluminum-containing adjuvants. Vaccine 2003; 21:3011-8; PMID:12798645; http://dx.doi.org/10.1016/S0264-410X(03)00109-9
19. Iyer S, Robinett RSR, HogenEsch H, Hem SL. Mechanism of adsorption of hepatitis B surface antigen by aluminum hydroxide adjuvant. Vaccine 2004; 22:1475-9; PMID:15063571; http://dx.doi.org/10.1016/j.vaccine.2003.10.023
20. Weissburg RP, Berman PW, Cleland JL, Eastman D, Farina F, Frie S, Lim A, Mordenti J, Nguyen TT, Peterson MR. Characterization of the Mn Gp120 HIV-1 vaccine - antigen-binding to alum. Pharmaceut Res 1995; 12:1439-46; PMID:8584477; http://dx.doi.org/10.1023/A:1016266916893
21. Rinella JV, White JL, Hem SL. Effect of pH on the elution of model antigens from aluminum-containing adjuvants. J Colloid Interf Sci 1998; 205:161-5; PMID:9710509; http://dx.doi.org/10.1006/jcis.1998.5648
22. Greiner VJ, Ronzon F, Larquet E, Desbat B, Esteves C, Bonvin J, Gréco F, Manin C, Klymchenko AS, Mély Y. The structure of HBsAg particles is not modified upon their adsorption on aluminium hydroxide gel. Vaccine 2012; 30:5240-5; PMID:22705175; http://dx.doi.org/10.1016/j.vaccine.2012.05.082
23. Rinella JV, Workman RF, Hermodson MA, White JL, Hem SL. Elutability of proteins from aluminum-containing vaccine adjuvants by treatment with surfactants. J Colloid Interf Sci 1998; 197:48-56; PMID:9466843; http://dx.doi.org/10.1006/jcis.1997.5230
24. Hutcheon CJ, Becker JO, Russell BA, Bariola PA, Peterson GJ, Stroop SD. Physiochemical and functional characterization of antigen proteins eluted from aluminum hydroxide adjuvant. Vaccine 2006; 24:7214-25; PMID:16860908; http://dx.doi.org/10.1016/j.vaccine.2006.06.043
25. Zhao Q, Potter CS, Carragher B, Lander G, Sworen J, Towne V, Abraham D, Duncan P, Washabaugh MW, Sitrin RD. Characterization of virus-like particles in GARDASIL (R) by cryo transmission electron microscopy. Hum Vacc Immunother 2014; 10:734-9; PMID:24299977; http://dx.doi.org/10.4161/hv.27316
26. Tang XH, Yang CY, Gu Y, Song CL, Zhang X, Wang YB, Zhang J, Hew CL, Li S, Xia N, et al. Structural basis for the neutralization and genotype specificity of hepatitis E virus. P Natl Acad Sci USA 2011; 108:10266-71; PMID:21642534; http://dx.doi.org/10.1073/pnas.1101309108
27. Zhang J, Gu Y, Ge SX, Li SW, He ZQ, Huang GY, Zhuang H, Ng MH, Xia NS. Analysis of hepatitis E virus neutralization sites using monoclonal antibodies directed against a virus capsid protein. Vaccine 2005; 23:2881-92; PMID:15780737; http://dx.doi.org/10.1016/j.vaccine.2004.11.065
28. Wei M, Zhang X, Yu H, Tang ZM, Wang K, Li Z, Zheng Z, Li S, Zhang J, Xia N, et al. Bacteria expressed hepatitis E virus capsid proteins maintain virion-like epitopes. Vaccine 2014; 32:2859-65; PMID:24662711; http://dx.doi.org/10.1016/j.vaccine.2014.02.025
29. Manek RV, Kunle OO, Emeje MO, Builders P, Rao GVR, Lopez GP, Kolling WM. Physical thermal and sorption profile of starch, obtained from Tacca leontopetaloides. Starch-Starke 2005; 57:55-61; http://dx.doi.org/10.1002/star.200400341
30. Zhao Q, Wang Y, Abraham D, Towne V, Kennedy R, Sitrin RD. Real time monitoring of antigenicity development of HBsAg virus-like particles (VLPs) during heat- and redox-treatment. Biochem Biophys Res Commun 2011; 408:447-53; PMID:21527246; http://dx.doi.org/10.1016/j.bbrc.2011.04.048
31. Zhao Q, Towne V, Brown M, Wang Y, Abraham D, Oswald CB, Gimenez JA, Washabaugh MW, Kennedy R, Sitrin RD. In-depth process understanding of RECOMBIVAX HB(R) maturation and potential epitope improvements with redox treatment: multifaceted biochemical and immunochemical characterization. Vaccine 2011; 29:7936-41; PMID:21871939; http://dx.doi.org/10.1016/j.vaccine.2011.08.070
32. Zhao Q, Modis Y, High K, Towne V, Meng Y, Wang Y, Alexandroff J, Brown M, Carragher B, Potter CS, et al. Disassembly and reassembly of human papillomavirus virus-like particles produces more virion-like antibody reactivity. Virol J 2012; 9:52; PMID:22356831; PMID:22356831; http://dx.doi.org/10.1186/1743-422X-9-52
33. Deschuyteneer M, Elouahabi A, Plainchamp D, Plisnier M, Soete D, Corazza Y, Lockman L, Giannini S, Deschamps M. Molecular and structural characterization of the L1 virus-like particles that are used as vaccine antigens in Cervarix (TM), the AS04-adjuvanted HPV-16 and-18 cervical cancer vaccine. Hum Vaccines 2010; 6:407-19; PMID:20953154; http://dx.doi.org/10.4161/hv.6.5.11023
34. Robert DS, Qinjian Z, Clinton SP, Bridget C, Washabaugh MW. Recombinant protein based viral vaccines, In Vaccine Analysis: Strategies, Principles and Control. (Chapter 3) Brian N et al. eds. Springer-Verlag Berkub Heidelberg, 2015; 81–112; http://dx.doi.org/10.1007/978-3-662-45024-6-3
35. Chang MF, Shi Y, Nail SL, HogenEsch H, Adams SB, White JL, Hem SL. Degree of antigen adsorption in the vaccine or interstitial fluid and its effect on the antibody response in rabbits. Vaccine 2001; 19:2884-9; PMID:11282199; http://dx.doi.org/10.1016/S0264-410X(00)00559-4
36. Iyer S, HogenEsch H, Hem SL. Relationship between the degree of antigen adsorption to aluminum hydroxide adjuvant in interstitial fluid and antibody production. Vaccine 2003; 21:1219-23; PMID:12559801; http://dx.doi.org/10.1016/S0264-410X(02)00556-X
37. Shi Y, HogenEsch H, Hem SL. Change in the degree of adsorption of proteins by aluminum-containing adjuvants following exposure to interstitial fluid: freshly prepared and aged model vaccines. Vaccine 2001; 20:80-5; PMID:11567749; http://dx.doi.org/10.1016/S0264-410X(01)00313-9

38. Rinella JV, White JL, Hem SL. Effect of anions on model aluminum-adjuvant-containing vaccines. J Colloid Interf Sci 1995; 172:121-30; http://dx.doi.org/10.1006/jcis.1995.1233
39. Shank-Retzlaff M, Wang F, Morley T, Anderson C, Hamm M, Brown M, Rowland K, Pancari G, Zorman J, Lowe R, et al. Research paper correlation between mouse potency and in vitro relative potency for human papillomavirus type 16 virus-like particles and Gardasil® vaccine samples. Hum Vaccines 2005; 1:191-7; http://dx.doi.org/10.4161/hv.1.5.2126
40. Zhao Q, Li S, Yu H, Xia N, Modis Y. Virus-like particle-based human vaccines: quality assessment based on structural and functional properties. Trends Biotechnol 2013; 31:654-63; PMID:24125746; http://dx.doi.org/10.1016/j.tibtech.2013.09.002
41. Tleugabulova D, Falcon V, Penton E. Evidence for the denaturation of recombinant hepatitis B surface antigen on aluminium hydroxide gel. J Chromatogr B, Biomed Sci Appl 1998; 720:153-63; PMID:9892077; http://dx.doi.org/10.1016/S0378-4347(98)00425-3
42. Gupta RK, Chang AC, Griffin P, Rivera R, Siber GR. In vivo distribution of radioactivity in mice after injection of biodegradable polymer microspheres containing 14C-labeled tetanus toxoid. Vaccine 1996; 14:1412-6; PMID:8994315; http://dx.doi.org/10.1016/S0264-410X(96)00073-4
43. Weissburg RP, Berman PW, Cleland JL, Eastman D, Farina F, Frie S, Lim A, Mordenti J, Nguyen TT, Peterson MR. Characterization of the MN gp120 HIV-1 vaccine: antigen binding to alum. Pharm Res 1995; 12:1439-46; PMID:8584477; http://dx.doi.org/10.1023/A:1016266916893
44. Mulder AM, Carragher B, Towne V, Meng Y, Wang Y, Dieter L, Potter CS, Washabaugh MW, Sitrin RD, Zhao Q. Toolbox for non-intrusive structural and functional analysis of recombinant VLP based vaccines: a case study with Hepatitis B vaccine. Plos One 2012; 7 (4):e33235; PMID:22493667; http://dx.doi.org/10.1371/journal.pone.0033235
45. Shank-Retzlaff ML, Zhao Q, Anderson C, Hamm M, High K, Nguyen M, Wang F, Wang N, Wang B, Wang Y, et al. Evaluation of the thermal stability of Gardasil (R). Hum Vaccines 2006; 2:147-54; http://dx.doi.org/10.4161/hv.2.4.2989
46. Schofield T. In virto versus in vivo concordance: a case study of the replacement of an animal potency test with an immunochemical assay. In: Karger BF (ed) Advancing Science and Elimination of the Use of Laboratory Animals for Development and Control of Vaccines and Hormones, 2002; 111:299-304.
47. Metz B, Hendriksen CFM, Jiskoot W, Kersten GFA. Reduction of animal use in human vaccine quality control: opportunities and problems. Vaccine 2002; 20:2411-30; PMID:12057596; http://dx.doi.org/10.1016/S0264-410X(02)00192-5
48. van der Kamp MD. Replacement, reduction or refinement of animal use in the quality control of veterinary vaccines: development, validation and implementation. Dev Biol Stand 1996; 86:73-6; PMID:8785994